Food Chemistry 297 (2019) 125005

Contents lists available at ScienceDirect

Food Chemistry

journal homepage: www.elsevier.com/locate/foodchem

Carbon nanotubes molybdenum disulfide 3D nanocomposite as novel nanoscaffolds to immobilize *Lens culinaris* β-galactosidase (*Lsbgal*): Robust stability, reusability, and effective bioconversion of lactose in whey

Anjali Yadav[a,1], Sumit Kumar Pandey[b,1], Dinesh Chand Agrawal[a], Himanshu Mishra[b], Anchal Srivastava[b,*], Arvind M. Kayastha[a,*]

[a] School of Biotechnology, Institute of Science, Banaras Hindu University, Varanasi 221005, India
[b] Department of Physics, Institute of Science, Banaras Hindu University, Varanasi 221005, India

ARTICLE INFO

Keywords:
Nanocomposite
MWCNT-MoS_2 NC
Lens culinaris
β-Galactosidase
Immobilization
Nanobiocatalyst

ABSTRACT

Multiwalled carbon nanotubes molybdenum disulfide 3D nanocomposite (MWCNT-MoS_2 NC) was successfully synthesized *via* eco-friendly hydrothermal method. The microstructural characterization of synthesized nanocomposite was carried out using different spectroscopic and microscopic techniques. Nanocomposite was activated using glutaraldehyde chemistry and used as a platform to immobilize *Lens culinaris* β-galactosidase (*Lsbgal*) which resulted in 93% of immobilization efficiency. Attachment of *Lsbgal* onto nanocomposite was confirmed by AFM, FE-SEM, FTIR, and CLSM. The nanobiocatalyst showed broadening in operational pH and temperature working range. Remarkable increase in thermal stability was observed as compared to soluble enzyme. Nanobiocatalyst showed outstanding increase in storage stability, retained 92% of residual activity over a period of 8 months. This offers good reusability as it retained ~50% residual activity up to 21 reuses and exhibited higher rate of lactose hydrolysis in whey. MWCNT-MoS_2 NC conjugated to biomolecules can serve as a potential platform for fabrication of lactose biosensor.

1. Introduction

Lactose sugar is one of the valuable assets of basic nutrients as it plays a crucial role in growth of animal during early stages of development. It influences the absorption of calcium, phosphorous, magnesium, and also helps in promoting the growth of acidic microflora of intestinal tract (Atkinson, Kratzer, & Stewart, 1957). However, when the consumption of lactose exceeds over the hydrolyzing capacities of β-galactosidase present in the gut, then symptom of lactose intolerance like abdominal pain, bloating, flatulence, vomiting, etc. arise (Shukla & Wierzbicki, 1975). The decrease in residual activity of β-galactosidase with the onset of ageing affects nearly 70% of world population (Adam, Rubio-Texeira, & Polaina, 2005). Thus, lactose intolerant people start avoiding milk and dairy products which later results in diseases like osteoporosis, cataract, and galactosemia.

In dairy industry β-galactosidase plays a crucial role in production of lactose reduced/free products by hydrolyzing lactose into glucose and galactose that improves the sweetness, and flavor of the dairy products (Richmond, Gray, & Stine, 1981). Nowadays, the production of Galacto-oligosaccharide (GOS) *via* transgalactosylation reaction by β-galactosidase has become popular because of its extraordinary nutraceutical and pharmaceutical properties that helps in the maintenance of microenvironment of the gut by restoring the growth of beneficial bacteria (Mahoney, 1998).

Besides milk, cheese whey is another major source of lactose sugar as it constitutes about 5–6% of the total whey. Earlier, González Siso (1996) had reported that manufacturing of 1 kg cheese produces 9 L of whey as waste. When the large quantity of lactose containing whey is dumped into water bodies, it increases the biological oxygen demand (BOD) and chemical oxygen demand (COD) (Geiger et al., 2016), leading major environmental concern. Lactose being a high calorie (energy) food cannot be dumped into waste stream.

Abbreviations: *Lsbgal*, *Lens culinaris β-galactosidase*; MWCNT-MoS_2 NC, Multiwalled carbon nanotubes molybdenum disulphide nanocomposite; NBCs, Nanobiocatalyst; FE-SEM, Field Emission-Scanning Electron Microscopy; TEM, Transmission Electron Microscopy; CLSM, Confocal Laser Scanning Microscopy; FTIR, Fourier Transformed Infrared Spectroscopy; AFM, Atomic Force Microscopy; RSM, Response Surface Methodology

* Corresponding authors.
E-mail addresses: anchalbhu@gmail.com (A. Srivastava), kayasthabhu@gmail.com (A.M. Kayastha).
[1] Authors contributed equally.

https://doi.org/10.1016/j.foodchem.2019.125005
Received 4 February 2019; Received in revised form 6 June 2019; Accepted 12 June 2019
Available online 12 June 2019
0308-8146/

Enzyme catalysis has been directed towards green synthesis and sustainable industrial technologies due to their non-hazardous and non-toxic nature because enzymes are produced from renewable resources and are biodegradable. They also catalyse the reaction with high specificity, efficiency, selectivity and also requires low energy input (Wohlgemuth, 2010). However, soluble enzymes are too expensive to be discarded after single use and often tend to loose activity at industrial conditions which are drastically different than the natural cellular environment of soluble biocatalyst in terms of pH, temperature, organic solvents, shearing forces, and product inhibition. To overcome above inadequacies, immobilization of enzymes on insoluble matrix has become a potential technology as it not only allow reuses the expensive biocatalyst with efficient recovery but also enhances the biocatalytic efficiency, stability, and prevents product inhibition (DiCosimo, McAuliffe, Poulose, & Bohlmann, 2013).

The multipoint covalent attachment of enzyme on a functionalized support *via* linker and the functional groups present on surface of enzyme induces the rigidity to the enzyme structure that enhances the stability of enzyme. However, multimeric enzyme are very susceptible to denaturation in many occasions, by dissociation of its subunits that may further contaminate the final products. Multisubunit attachment of multimeric enzyme through multipoint attachment/covalent attachment on functionalized support tremendously improves the stability of enzyme under extreme conditions (Mateo, Palomo, Fernandez-Lorente, Guisan, & Fernandez-Lafuente, 2007). As a result of immobilization it also reduces the affinity for inhibitors to produce inhibition by distorting/blocking the interaction site other than active site in case of allosteric inhibitor, and active site in case of competitive inhibition (Rodrigues, Ortiz, Berenguer-Murcia, Torres, & Fernandez-Lafuente, 2013). Immobilization has become a potential tool to boost enzyme selectivity or specificity. It is merely a process which relies on the possibilities of creating library of immobilized enzyme that contains the enzyme highly selective for one enantiomer and other preparation is highly selective toward the other isomer (Rodrigues et al., 2013).

Nowadays, advancement in nanotechnology has offered various nanoscale material to be more accessible to a wide range of applications in field of bio-imaging, nano-medicine, drug delivery, and in biomedical implementation (Kim, Grate, & Wang, 2008). Recently, graphene, graphene oxide, iron oxide, carbon nanotubes (CNTs) have attracted attention because of their larger surface area with faster electrode kinetics making them promising candidate for biosensor fabrications (Liu, Yu, Zeng, Miao, & Dai, 2010; Shan et al., 2009; Singh et al., 2018). Earlier, we have reported successful immobilization of β-amylase on MoS_2 nanosheets (MoS_2 NSs) with 92% immobilization efficiency (Das, Mishra, Srivastava, & Kayastha, 2017). However, these two dimensional (2D) nanosheets suffers from the problem of re-stacking that reduces the surface to volume ratio and hence, reduces the enzyme loading capacities (Shouzhi et al., 2017).

In order, to overcome the problem of re-stacking of 2D nanomaterials, 3D nanocomposite has been synthesized, where molybdenum disulphide (MoS_2) nanosheets (2D) have been grown on the multiwalled carbon nanotubes (MWCNTs).The support of MoS_2 NSs over MWCNTs resist the restacking of nanosheets. L-Cysteine assisted synthesis of MWCNT-MoS_2 NC by hydrothermal method has attracted the attention of many researchers as L-cysteine possess multifunctional groups ($-NH_2$, $-SH$, and $-COOH$). L-cysteine acts as a source of sulphur and helps to grow MoS_2 NSs over the surface CNTs. Chou et al. (2013) have demonstrated that thiol group of L-cysteine coordinated to Mo atoms at S-vacancies while amine and carboxylic group remain free. Many authors have confirmed the presence of amino functional groups on the surface of MoS_2 NSs synthesized using L-cysteine as source of sulphur (Veeramalai, Li, Xu, Kim, & Guo, 2015; Wang & Ni, 2014). Earlier, Talat, Awasthi, Sundar, and Srivastava (2015) have used L-cysteine to amino functionalize various carbon-nanomaterial such as graphene and CNTs. Heterofunctional support has opened new opportunities for enzyme immobilization. Various functional groups present on the surface of NC, help in adsorbing the protein physically and subsequently, form covalent bond with functional group present on the enzyme surface. This allows the enzyme to orient in different zones in its surface (Barbosa et al., 2013; Melo et al., 2017) that result in intense multipoint covalent attachment. While in case of monofunctional support it will orient in the direction where high density of lysine group would be present. The later one reduces the multipoint covalent attachment. Recently, Zaak, Sassi, and Fernandez-Lafuente (2018) have shown successful immobilization of *Aspergillius oryzae* β-galactosidase on heterofunctional support (amine-vinyl sulfone) whereas same enzyme could not be immobilized onto vinylsulfone support.

Glutaraldehyde is an inexpensive, non-toxic bi-functional reagent and widely used in enzyme immobilization because of its solubility in aqueous medium. It exists in monomeric, polymeric form in aqueous solution which remain in equilibrium with each other. It reacts primarily with the amino functional group of enzyme but it can also react with other functional groups such as thiol, phenol, and imidazole. Under acidic and neutral conditions, aldehyde groups present on glutaraldehyde react with two lysine groups on the enzyme surface, resulting in the formation of Schiff base, which is stable to acid hydrolysis (Barbosa et al., 2014). The main reason behind stability of the product is resonance interaction of Schiff base with ethylenic double bond. Monsan (1978) has documented the influence of several parameters such as support porosity, glutaraldehyde concentartion, time of action and pH for the activation of amine group on porous silica with glutaraldehyde. Xiao, Xie, Militz, and Mai (2010) have documented that aldehyde group of glutaraldehyde react with hydroxyl groups to form hemiacetal and requires two hydroxyl group to form acetal. Previously, β-galactosidase from different sources have been immobilized onto various nanoparticles. Pan et al. (2009) have immobilized *Aspergillus oryzae* β-galactosidase onto magnetic-Fe_3O_4 chitosan nanoparticles by covalent attachment using glutaraldehyde as an activating agent and showed successful synthesis of GOS 15.5% (w/v) when 50% of lactose was hydrolysed. Recently, Khan, Husain, and Bushra (2017) have immobilized β-galactosidase on surface modified cobalt multiwalled carbon nanotubes nanocomposites by physical adsorption/covalent attachment. The result showed improved stability and resistance to inhibitors. To the best of our knowledge, this is the first report of immobilization of *Lens culinaris* β-galactosidase onto MWCNT-MoS_2 NC.

In the present work, functionalized 3D MWCNT-MoS_2 NC has been successfully synthesized *via* single-step hydrothermal route, which is facile, eco-friendly, and economical. Characterization of the functionalized MWCNT-MoS_2 NC was done using different spectroscopic and microscopic techniques. Thereafter NC was activated using glutaraldehyde as an activating agent and *Lens culinaris* β-galactosidase (*Lsbgal)* was immobilized onto it [Scheme 1]. Attachment of *Lsbgal* onto MWCNT-MoS_2 NC was confirmed by Field Electron-Scanning Electron Microscopy (FE-SEM), Atomic Force Microscopy (AFM), Fourier Transformed Infrared Spectroscopy (FTIR) and Confocal Laser Scanning Microscopy (CLSM). A comparative study between soluble and immobilized *Lsbgal* has been carried out w.r.t. pH, temperature, thermal stability, kinetic parameters and product inhibition.

2. Materials and methods

2.1. Materials

Lens culinaris (Lentils) seeds were procured from agriculture seed store. All chemicals for preparing buffer were of analytical grade and purchased from Merck Eurolab GmbH Darmstadt, Germany. For the synthesis of MWCNTs hydrocarbon, toluene (C_7H_8) and catalyst ferrocene ($C_{10}H_{10}Fe$) were procured from Hi-Media, India. Sodium molybdate dihydrate ($Na_2MoO_4.2H_2O$) and L-cysteine were purchased from Molychem, India. Rest of the chemical were purchased from Sigma (USA). Milli Q (MQ) water (Millipore, Bedford, MA) with resistance > 18 MΩ.cm was used throughout the experiment.

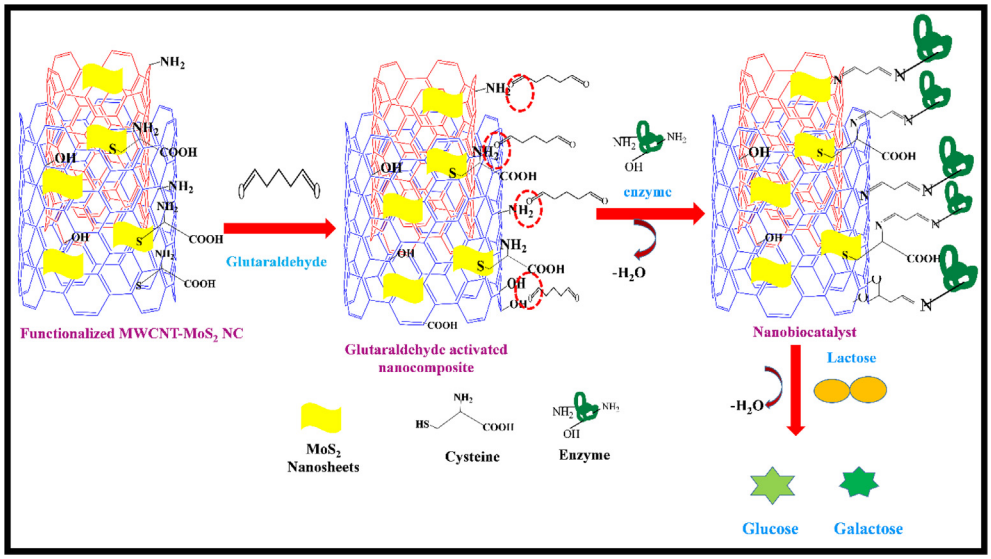

Scheme 1. Overall scheme of immobilization of *Lsbgal* onto functionalized MWCNT-MoS_2 NC producing nanobiocatayst (NBCs) for lactose based dairy industries.

2.2. Enzyme extraction

All the experiments were carried out at 4 °C and centrifugation at 8720g, unless stated otherwise.

Lens culinaris (50 g) seeds were soaked overnight, crushed using Waring blender in chilled extraction buffer (pH 6.7, 25 mM, sodium phosphate buffer). Thereafter, squeezed with pre-washed double-layered muslin cloth, and subsequently centrifuged for 20 min to remove cell debris. The supernatant was subjected to acetone precipitation in range of 35–55% at −17 °C. Subsequently, obtained enzyme was subjected to ammonium sulphate fractionation in range of 35–55% at 4 °C. Enzyme was further purified by hydrophobic interaction chromatography i.e. Octyl-Sepharose-4B and followed by Size-Exclusion Chromatography on Superdex-200 (GE Healthcare) on AKTA purifier. The final purified enzyme was used throughout experiment for immobilization studies.

2.3. Protein estimation

The protein estimation has been done by following Bradford method using Bovine Serum Albumin (BSA) as standard (Bradford, 1976).

2.4. Enzyme assay

2.4.1. Soluble Lsbgal assay

Activity of soluble and immobilized *Lsbgal* against ortho-nitrophenyl-β-D-galactopyranoside (ONPG) and lactose as substrate was monitored by following published procedure (Kishore, Talat, Srivastava, & Kayastha, 2012). Briefly, activity of soluble *Lsbgal* against ONPG was assayed in final volume of 500 µl, with 50 mM of glycine-HCl buffer (pH 3.0) containing 20 mM of ONPG and 10 µl of diluted enzyme, incubated at 58 °C for 10 min. The reaction was stopped by adding 1.5 mL of sodium-tetraborate (20 mM) and end product i.e. ortho-nitrophenolate was measured spectrophotometrically (UV–Visible double beam spectrophotometer (JASCO ETC-717, Japan) at 405 nm. One unit is defined as one µmol of *o*-nitrophenolate formed per min by the amount of enzyme under standard assay conditions (extinction coefficient (ε) for *o*-nitrophenolate was 4050 $M^{-1}cm^{-1}$).

Activity measurement against lactose as a substrate was assayed in 50 µl of reaction mixture (50 mM sodium acetate buffer, pH 4.0 and 50 mM of lactose) using diluted enzyme (10 µl) to reaction mixture and incubating it for 10 min at 55 °C. Further, reaction was stopped by heating in boiling water bath (Pharmacia MultiTemp II, Sweden) for 5 min, and the released glucose was estimated by GOD-POD method (Commercially available kit by Span Diagnostic Ltd., Surat, India). The 20 µl of the above reaction mixture was added to 500 µl of glucose reagent, and change in absorbance was monitored at 505 nm. The concentration of glucose present in the sample was calculated by using the formula:

$$\text{Glucose(mg/ml)} = \text{Absorbance of test sol.} / \text{Absorbance of standard sol.}$$

One unit of β-galactosidase is defined, as the amount of enzyme required to release one µmol of glucose per min at 55 °C, under standard conditions.

During immobilization on MWCNT-MoS_2 NC, *Lsbgal* activity was monitored against ONPG due to their higher sensitivity than lactose. Immobilization efficiency was calculated using the following formula:

$$\text{Immobilization efficiency (\%)} = \frac{\text{Specific activity of immobilized } Lsbgal}{\text{Specific activity of soluble } Lsbgal} \times 100$$

For calculation of immobilization efficiency, specific activity of soluble and immobilized *Lsbgal* were 87 U/mg and 81 U/mg, respectively.

2.5. Synthesis of MWCNT-MoS_2 nanocomposite (MWCNT-MoS_2 NC)

2.5.1. Synthesis of Multi-walled carbon nanotubes (MWCNTs)

MWCNTs were synthesized by a single step spray pyrolysis technique using ferrocene ($C_{10}H_{10}Fe$) as a catalyst and toluene (C_7H_8) as a hydrocarbon source. In brief, a mixture of ferrocene and toluene with certain amount of catalyst to source ratio were injected inside a quartz tube of length 70 cm and of inner diameter 2.7 cm, which was heated up to 850 °C under the constant flow of argon (Ar) gas and then allowed to cool down to room temperature. The thick black MWCNTs deposited on the inner walls of the reactor quartz tube was collected (Srivastava, Srivastava, Talapatra, Vajtai, & Ajayan, 2004).

2.5.2. Hydrothermal synthesis of MWCNT-MoS_2 NC

The MWCNT-MoS_2 NC was prepared by the facile and eco-friendly hydrothermal route by following published procedure (Das et al., 2017). Briefly, $Na_2MoO_4.2H_2O$ (0.25 g) was dissolved in 25 mL of deionized (DI) water, and stirred for 10 min at 40 °C. In a separate beaker, 0.50 g of L-cysteine was dissolved in 50 mL of Milli Q water and stirred for 10 min at 40 °C. Thereafter, both the solutions were mixed and stirred for 10 min at 40 °C. During the process, HCl (0.1 N) added to the solution to maintain its pH approximately at 5.0 and then MWCNTs

(0.50 g) were added into the solution and ultrasonically dispersed in it. The mixture was autoclaved at 200 °C for 48 h. After cooling to room temperature the resulting black precipitate was washed 2–3 times with Milli Q water, and dried at 65 °C for 12 h. The overall process has been described in the supplementary file [Scheme S1].

2.6. Enzyme immobilization

L-Cysteine assisted synthesis of MWCNT-MoS_2 NC *via* hydrothermal route results in functionalization of nanocomposite with different groups such as $-NH_2$, $-COOH$ and $-OH$. Thereafter, functionalized MWCNT-MoS_2 NC has been activated using glutaraldehyde bifunctional reagent, followed by immobilization as described earlier (Das et al., 2017). In brief, functionalized MWCNT-MoS_2 NC of (1 mg/ml), dispersed in sodium acetate buffer at (50 mM, pH 5.5), sonicated for 20 min. The obtained homogenous solution was further divided in 29 aliquots as stated in Box-Benhken Design (BBD) [Table S1]. These aliquots were centrifuged at 4000 rpm for 5 min, incubated with glutaraldehyde for 4 h in dark at room temperature. Thereafter, washed with sodium acetate buffer (50 mM, pH 5.5) to remove excess of glutaraldehyde and further incubated with enzyme, overnight at 4 °C. Following day, unbounded proteins were removed by washing twice with chilled sodium acetate buffer (50 mM, pH 5.5). Finally, activity of bound enzyme was estimated. All the experiments, were performed in duplicates, and their average was taken to calculate immobilization (%).

2.7. Experimental setup and statistical analysis

Initially, we performed experiments at broader range and optimized one parameter at a time while keeping other parameters constant such as pH (3.0–7.0), glutaraldehyde (1–7%; v/v), amount of nanocomposite (200–2500 μg), and amount of *Lsbgal* (20–500 μg). Activity was monitored using ONPG over the period of one week to get maximum activity and stability. Thereafter, experiments were performed at narrow range, and the preparations having highest activity were selected and optimized using BBD (Design Expert 11, Minneapoils, USA). In this study, experimental design consist of 29 trials of experiments. The independent variables and their level selected for obtaining maximum immobilization of *Lsbgal* onto functionalized MWCNT-MoS_2 NC are as follows: amount of MWCNT-MoS_2 NC (500 μg, 1000 μg, and 1500 μg), amount of enzyme (50 μg, 100 μg, and 150 μg), (%; v/v) glutaraldehyde (1.5, 3.0, 4.5), pH (5.0, 5.5, 6.0). All the experiment were performed in duplicates and there average was taken to calculate the immobilization (%) or response (Y). The quadratic polynomial equation has been employed to calculate mathematical relationship relating to different variables are as follows:

$$Y_i = \beta_o + \sum \beta_i X_i + \sum \beta_{ii} X_i^2 + \sum \beta_{ij} X_i X_j$$

Y_i is predicted response, X_iX_j are input variables, which affects the response variable Y; β_o is the offset term; β_i shows linear coefficient, β_{ii} is the quadratic coefficient and β_{ij} coefficient term. In order to check adequacy of model, coefficient of determination (R^2) and adjusted R^2 values were evaluated. To evaluate the fitness of model with polynomial equation, analysis of variance (ANOVA), a statistical tool was performed which included several parameters such as Lack of fit, p-value, and model F-value. The generated model was validated by conducting experiments at given optimal conditions.

2.8. Characterization

The microstructural characterization of the synthesized MWCNTs and MWCNT-MoS_2 NC were performed using X-ray diffractometer (XRD, Philips Pan analytical X'Pert Pro). Brunauer-Emmett-Teller (BET) surface area was analyzed by nitrogen (N_2) adsorption-desorption isotherms measured at 77 K with Qantachrome Instruments (model: As-iQ-C (P/N: 62143-iTCD), USA. To observe the morphology of the MWCNTs samples, Scanning Electron Microscopy (SEM) (SEM, Zeiss Germany), Transmission Electron Microscopy (TEM) (TECNAI 20 G^2) operated at accelerating voltage of 200 kV was used. Energy dispersive X-ray spectroscopy (EDS) has been employed to analyze the elemental composition of the MWCNT-MoS_2 NC. The spectroscopic characterization of the MWCNT-MoS_2 NC was carried out using Raman spectroscopy (Renishaw inVia, Germany). In order to confirm the immobilization of *Lsbgal* on MWCNT-MoS_2 NC, FTIR of MWCNTs, bare MWCNT-MoS_2 NC, glutaraldehyde treated MWCNT-MoS_2 NC, and *Lsbgal* immobilized MWCNT-MoS_2 NC was carried out using Fourier-transform infrared (FTIR) spectrometer (Frontier, Perkin Elmer, USA) in attenuated total reflectance (ATR) mode.

FE-SEM (Nova Nano 450, FEI) has been employed to observe the morphological changes before and after immobilization. AFM (NT-MDT, NTEGRA PRIMA) with scanning speed of 0.5 Hz in semi-contact mode equipped with silicon tip has been carried out to access the topology of native MWCNT-MoS_2 NC and *Lsbgal* immobilized onto MWCNT-MoS_2 NC. In order to get insight of the distribution of enzyme within support (nanocomposite), confocal laser scanning microscopy (CLSM) (Carl Zeiss 800) has been carried out to detect the fluorescence signal for fluorescence isothiocyanate isomer I (FITC) labeled enzyme, before and after immobilization. The FITC labeling of *Lsbgal* has been carried out in following manner: FITC solution (0.5 mg/ml) was prepared by dissolving in minimum volume of dimethyl sulfoxide (DMSO) and the rest of the volume was made up by Tris-HCl buffer (pH 8.5, 50 mM). Approximately 50 μl of FITC was added to bare MWCNT-MoS_2 NC and *Lsbgal* immobilized onto MWCNT-MoS_2 NC, incubated for 30 min in dark and unbound FITC was removed by washing with MQ water. The samples were excited at wavelength of 390 nm and emission spectra were recorded at 490 nm.

2.9. Steady state kinetics

2.9.1. pH-activity profile

The determine the effect pH on the activity of *Lsbgal* (both soluble and immobilized) was studied against ONPG in pH range 3.0–7.0 using following buffers: glycine-HCl 3.0–4.0 (50 mM), acetate buffer 4.0–5.5 (50 mM), sodium phosphate 6.0–7.0 (50 mM).

2.9.2. Temperature-activity profile

To determine the effect of temperature on the activity of *Lsbgal* (soluble and immobilized), activity was monitored in range of 25 °C–75 °C by assaying the enzyme activity at its optimum pH for 10 min.

2.9.3. Determination of thermal stability

The thermal stability was studied by pre-incubating the soluble and immobilized enzymes at various temperature for different time intervals. Aliquots were withdrawn at regular intervals and followed by residual activity assay under standard experimental conditions.

2.9.4. Determination of kinetic parameters

The kinetic parameters K_m *and* V_{max} of the soluble and immobilized enzyme was determined by varying the substrate concentration i.e. ONPG from 0.2 mM to 40 mM in pH 3.0 (Gly-HCl buffer, 50 mM) at 58 °C, under standard assay conditions. While for lactose, varying concentration (2–40 mM) in pH 4.5 (sodium acetate buffer, 50 mM) at 55 °C. Data were evaluated and plotted using Lineweaver-Burk Plot with the help of Sigma Plot Version 11.0.

2.9.5. Determination of reusability

In order to determine reusability, stored nanobiocatalyst (NBCs) were used repeatedly for more than 21 times within 96 h for assessment of residual activity against ONPG and lactose as a substrate. After each

activity measurement the immobilized enzyme was washed twice with sodium acetate buffer (50 mM, pH 5.5) to remove excess substrates. The activity obtained after first cycle was taken as control (100%). All the experiments were performed in triplicates and their average was taken to calculate the residual activity.

2.9.6. Determination of storage stability

The aliquots of NBCs were stored in both dry and wet conditions (sodium acetate buffer, 50 mM, pH 5.5) at room temperature and 4 °C, respectively, along with purified *Lsbgal* stored at 4 °C. Residual activity was checked regularly at different time intervals with ONPG taken as a substrate under standard experimental conditions.

2.10. Lactose and whey hydrolysis

Milk and whey were prepared as stated earlier (Dwevedi & Kayastha, 2009). Natural whey was centrifuged for 5 min at 10,000 rpm and obtained supernatant was used for experiment. NBCs (1 mg), were incubated with milk, whey, and natural whey separately at room temperature on shaker incubator at 80 rpm for 24 h. Aliquots were withdrawn at regular interval (0–24 h), for the assessment of glucose released. Glucose measurement has been carried out by procedure described in enzyme assay section.

2.10.1. Effects of glucose and galactose

The activity of soluble and immobilized *Lsbgal* was assayed independently with increasing concentration of galactose (1–50 mM) and glucose (1–100 mM) in Gly-HCl buffer (pH 3.0, 50 mM) at 58 °C. The activity in absence of galactose and glucose was taken as control (100%) for calculation of residual (%) of activity.

3. Results and discussion

Lsbgal was purified 857-fold from *Lens culinaris* seeds by applying precipitation and chromatographic techniques. When purified enzyme was subjected to electrophoresis on an acrylamide in the presence of SDS, hetero-dimeric bands with apparent molecular mass of 40 kDa and 35 kDa were observed. *Lsbgal* has K_m and V_{max} values 1.21 mM and 90.90 μmoles/min/mg for ONPG, respectively. The purified enzyme was optimally active at pH 3.0 and 58 °C, respectively (unpublished results).

3.1. Microstructural and morphological characterization

Structural confirmation of MWCNTs and MWCNT-MoS_2 NC were studied using X-ray diffraction (XRD). The XRD spectrum [Fig. S1(a)] for MWCNTs and MWCNT-MoS_2 NC, were showed in black and red color, respectively. XRD peaks corresponding to the MWCNTs have been successfully indexed using JCPDS Card no. 75-1621. Peaks appearing at positions 26.09°, 44.10°, 54.04°, 77.79° corresponds to the (0 0 2), (1 0 1), (0 0 4) and (1 1 0) planes of the MWCNTs, respectively. A small peak at position 44.66° (JCPDS Card no. – 65-5099) also appears that may be attributed to the Fe present within the MWCNTs which was used as catalyst during synthesis of nanotubes. In the XRD spectra of MWCNT-MoS_2 NC, additional peaks corresponding to the 2H-MoS_2 appear and indexed successfully using JCPDS Card no. 77-1716. XRD peaks at positions 13.10°, 31.80°, 32.99°, 56.44°, 58.15° and 66.25° correspond to (0 0 2), (0 0 4), (1 0 0), (1 0 6) and (2 0 4) of 2H-MoS_2 while peaks appearing at 27.20°, 45.52° and 46.30° may be assigned to the residual oxide impurities of molybdenum (MoO_3).

It is well-known that Raman spectra are the fingerprint for any material and is non-destructive technique. Therefore, for further structural confirmation, Raman spectra of MWCNTs and MWCNT-MoS_2 NC have been recorded [Fig. S1(b)]. Raman spectra of MWCNTs consists of D band at 1350 cm^{-1} corresponding to the scattering from local defects or disorders present in MWCNTs. The G band at 1583 cm^{-1} is due to the in-plane tangential vibration of C—C bonds (Lehman, Terrones, Mansfield, Hurst, & Meunier, 2011). Similarly for MWCNT-MoS_2 NC typical D and G band of MWCNTs are found at the same wavenumber as for MWCNTs, however, two additional peaks appear at ~383 cm^{-1} and 405 cm^{-1}, which correspond to the in plane (E^1_{2g}) and out of plane (A_{1g}) vibrational modes of MoS_2, respectively. E^1_{2g} mode originates from opposite vibration of two S atoms with respect to the Mo atom while the A_{1g} mode is the out-of-plane vibration of only S atoms in opposite directions. The wavenumber difference of (Δ) E^1_{2g} and A_{1g} is found to be ~23 cm^{-1}, which confirms the multilayer structure of MoS_2 NSs. Raman spectrum of the MWCNT-MoS_2 NC shows the characteristic bands of both MWCNTs and MoS_2, confirming the successful synthesis of the composite nanostructure. The surface area and pore radius of MoS_2 NSs and MWCNT-MoS_2 NC were investigated by N_2 adsorption-desorption isotherms measured at 77 K [Fig. S2(a) and (b)]. The observed BET surface area of MoS_2 NSs and MWCNT-MoS_2 NC are 4.406 m^2g^{-1} and 23.265 m^2g^{-1} respectively (approx. six times higher in case of MWCNTs MoS_2 NC). The Barrett-Joyner-Halenda (BJH) pore size distribution curve (inset) indicates that the pore size for the both MoS_2 NSs and MWCNTs MoS_2 NC are ~17 Å and ~15 Å, respectively. Thus, the MWCNT MoS_2 NC provides the more active surface area which would enhance the enzyme immobilization.

The morphology and microstructure of the MWCNTs and MWNCT-MoS_2 NC have also been investigated using TEM. TEM micrograph of MWCNTs revealed that the outer diameter was found to be 20–30 nm with the catalyst at its tip [Fig. 1(a)]. Fig. 1(b) shows the TEM image of MWCNT-MoS_2 NC in which at some places MoS_2 NSs are wrapped over MWCNTs (shown by blue dotted circles). It may be predicted that during the hydrothermal process, intrusion of MWCNTs serve as a nucleation centre for the growth of MoS_2 NSs. To observe the morphology

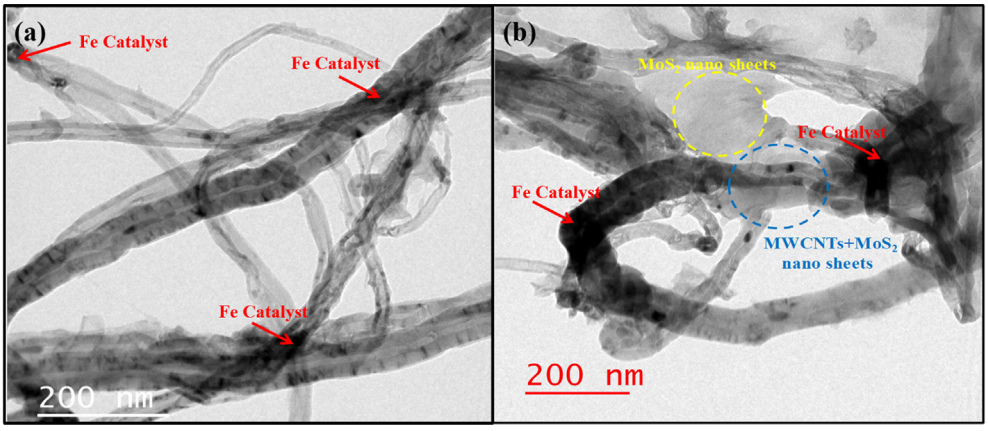

Fig. 1. TEM micrograph of (a) synthesized MWCNTs, (b) MWCNT-MoS_2 NC synthesized *via* hydrothermal method.

of MWCNT-MoS_2 NCs, SEM was performed in which the attachment of MoS_2 NSs is clearly visible [Fig. S3]. The elemental analysis of MWCNT-MoS_2 NC was also carried out by EDS, which showed sharp peaks of Mo, S, and C [Fig. S4]. Some additional peaks of Cu was also observed which may be due to Cu grid.

To understand the interaction between *Lsbgal* and MWCNT-MoS_2 NC, FTIR spectra of MWCNTs, bare MWCNT-MoS_2 NC, glutaraldehyde treated MWCNT-MoS_2 NC and *Lsbgal* immobilized MWCNT-MoS_2 NC were recorded [Fig. S5]. Absence of vibrational frequencies in case of MWCNTs confirmed that there is no functional group attached with carbon nanotubes [Fig. S5(a)]. However, vibrational frequency ~475 cm^{-1} in MWCNT-MoS_2 NC, correspond to Mo-S vibration of MoS_2 NSs (Das et al., 2017) [Fig. S5(b)]. Other vibrational frequencies such as at 720 cm^{-1}, 990 cm^{-1}, 1122 cm^{-1}, 1406 cm^{-1}, 1636 cm^{-1}, 2852 cm^{-1}, 2922 cm^{-1}, 3425 cm^{-1} correspond to N—H wag of primary amines, Mo-O vibrations, C—O stretching, N—H plane vibrations, N—H bend, dimer —OH and O—H stretching, and N—H stretching vibrations, respectively (Veeramalai et al., 2015). These vibrational frequencies confirmed the presence of -N and -O functionalities on MWCNT-MoS_2 NC. Next, the treatment of nanocomposite with glutaraldehyde leads to the binding of one arm of glutaraldehyde to the $-NH_2$ and —OH functional groups of nanocomposite and other arm remains free for the attachment with the $-NH_2$ groups of *Lsbgal*. Covalent bond (Schiff base) is responsible for the attachment of $-NH_2$ groups of *Lsbgal* with the —CHO group of glutaraldehyde. This binding of glutaraldehyde with MWCNT-MoS_2 NC has been confirmed by the vibrations of primary amines at 1636 cm^{-1} and also supported by strong stretching at 3425 cm^{-1} [Fig. S5(c)]. Finally, a shift in vibration frequencies was observed at 1639 cm^{-1} of FTIR spectrum, which confirmed the attachment of enzyme over the surface of nanocomposite. Subsequently, broad and intense stretching of peak at 3450 cm^{-1} also confirms the binding of enzyme over MWCNT-MoS_2 NC [Fig. S5(d)] (Deep et al., 2012). However, it was observed that the intensities of peak at 1639 cm^{-1} after covalent immobilization decreases, which can be due to strong covalent interactions between enzyme and nanocomposite. Previously, Khan et al. (2017) have also investigated similar decrease in the intensities of peak after covalent bond formation.

In order to get insights of morphological changes before and after immobilization of *Lsbgal* on MWCNT-MoS_2 NC, FE-SEM imaging was performed and obtained results are shown in [Fig. 2]. Fig. 2(a & c) represents the bare MWCNT-MoS_2 NC at resolutions 400 nm & 1 μm, respectively, where it appears as tube like structure onto which MoS_2 NSs attachment can be seen (highlighted with yellow dashed lines). It is clearly observed that these nanotubes were interconnected to each other while Fig. 2(b & d) represents *Lsbgal* immobilized MWCNT-MoS_2 NC in which translucent white patches of immobilized enzymes can be seen over the surface of MWCNT-MoS_2 NC at resolutions 400 nm & 1 μm, respectively (highlighted with yellow dashed line). Results obtained along with activity assay confirmed the immobilization.

In recent years, AFM has become a powerful tool because of its potential application in imaging and measuring matter at nanoscale level with high resolution. Therefore, to endorse immobilization through other ways, AFM was carried out to visualize surface topography before and after immobilization in tapping/semicontact mode as shown in [Fig. 3]. Fig. 3(a) & (b) represent the 2D and 3D images of MWCNTs-MoS_2 NC, which confirmed that the MWCNTs in the presence of MoS_2 NSs are well inter-connected. Further, [Fig. 3(c) & (d)] represent the AFM image of enzyme immobilized MWCNT-MoS_2 NC in which white patches appearing in the 2D image and in form of spikes in 3D image confirmed the presence of enzyme in random order but covering the complete scanning area (4 μm × 4 μm).

Confocal Laser Scanning Microscopy (CLSM) was performed to examine the distribution of enzymes onto MWCNT-MoS_2 NC as well as to confirm immobilization. Supplementary file Fig. S6(a) represents CLSM of native MWCNT-MoS_2 NC treated with FITC and Fig. S6(b) represents CLSM image after immobilization labeled with FITC. No fluorescence signal was observed in native nanocomposite, while Fig. S6(b) showed non-uniform distribution of fluorescence signal onto MWCNT-MoS_2 NC, which confirmed the attachment of enzyme over the surface of MWCNT-MoS_2 NC.

3.2. Optimization

Optimization is an essential parameter to obtain best performance of the system to design a process from the industrial view point because it does not only reduces the cost, time but also ease extensive laboratory work. Response Surface Methodology (RSM) consist of two designs i.e. BBD and Central Composite Design (CCD) which are commonly used to study the effect of various parameters on a system to get maximum performance of the system. However, in the present study we have used BBD because of its accuracy and better efficacy as compared to CCD (Bezerra, Santelli, Oliveira, Villar, & Escaleira, 2008). In order to ascertain maximum immobilization condition, experiments were designed within the described range, based on the preliminary results [Table S1] supplementary file. A contour and 3D plot was designed within a set of range and levels to get maximum immobilization [Fig. S7] and following points were resolute.

Amount of MWCNT-MoS_2 NCs: 1059.27 μg, amount of β-gal: 111.95 μg, glutaraldehyde (%; v/v): 3.57, pH 5.53. Immobilization: 92.35%

In order to ascertain the predicted 92.35% of immobilization efficiency, few experiments were carried out at given optimal conditions. Experimental validations for optimal immobilization were carried out and 93% of immobilization efficiency was achieved, which was in close agreement with predicted immobilization efficiency. Thus, predicted model was validated experimentally. Obtained results generated 3D model and contour plots, showing the effects of various parameter on response (immobilization efficiency) [Fig. S7]. Quadratic polynomial equation determines the relationship between immobilization efficiency and independent parameters. The equation representing actual factors affecting the immobilization are as follows:

Immobilization efficiency equation:

$$-1188.97283 + 0.036786 \times A + 465.68133 \times B - 13.59911 \times C - 0.091473 \times D - 0.003500\ A \times B + 0.002000\ A \times C - 0.000015\ A \times D + 4.40000\ B \times C + 0.022000\ B \times D + 0.023333\ C \times D - 0.000010 \times A^2 - 43.35133 \times B^2 - 2.07793 \times C^2 - 0.000425 \times D$$

where A is the amount of MWCNT-MoS_2 NC (μg); B is pH; C represents glutaraldehyde (v/v ; %); and D represents amount of enzyme (μg).

To check the adequacy and significance of the model ANOVA was performed [Table S2]. The "model F-value" 17.05 implies that model is significant and there is only 0.01% chance that may occur due to noise. However, F-value of Lack of fit 2.19 showed that lack of fit is not significant relative to pure error. Non-significant lack of fit is good for the model, which indicates this fits the model with superior precision. One significant parameter i.e. adequate precision measures the signal to noise ratio; ratio greater than 4 is required for good model and in the present model, adequate precision value is 14.56, which means this model can be used to navigate the design in space. Coefficients of determination (R^2) 0.9446 that indicates that model failed to explain only 5.54% of variations. However, Adjusted determination coefficient (Adj R^2) 0.8892 is in reasonable agreement with the predicted R^2 (Pred R^2) 0.7169 which confirms that the obtained models are significant.

3.3. Steady state kinetics

3.3.1. Effect of pH on activity

Immobilization of *Lsbgal* onto MWCNT-MoS_2 NC improves NBCs kinetic behaviour as compared to soluble *Lsbgal* by the microenvironment. Optimum pH of immobilized and soluble *Lsbgal* was determined in the pH range of 2.5–7.5 [Fig. 4(a)]. Optimum pH of immobilized

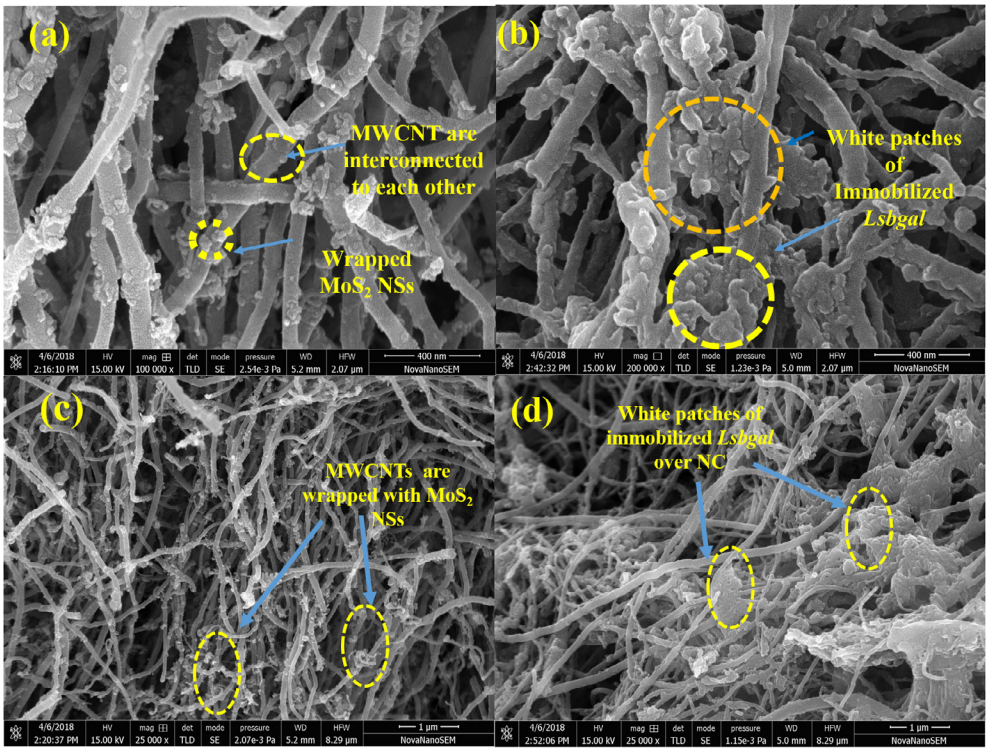

Fig. 2. FE-SEM micrograph at different resolutions (a) & (c) represents native MWCNT-MoS_2 NC, MWCNTs appears as a tube like structure onto which MoS_2 NSs are wrapped at 400 nm and 1 μm, respectively (b) & (d) shows white patches of immobilized enzyme on MWCNT-MoS_2 NC at 400 nm & 1 μm, respectively.

Lsbgal shifted from 3.0 to 3.5, with broadening of pH working range which indicates that NBCs has become flexible to pH changes as compared to soluble *Lsbgal*. Immobilized *Lsbgal* retained 65% of residual activity at pH 7.5 under mild alkaline condition while soluble *Lsbgal* retained only 22% of residual activity at same pH. The broadening of pH working range could be attributed to multisubunit multipoint covalent attachment, which increases the stability and prevent the dissociation of enzyme subunits. The shift in optimum pH depends upon the type of charge present on the surface of support and enzyme (Kishore et al., 2012). In present study, *Lsbgal* immobilized on MWCNT-MoS_2 NC showed better flexibility to pH changes, making it a promising candidate for industrial purpose.

3.3.2. *Effect of temperature on activity*

The NBCs showed one-degree shift in optimum temperature as compared to soluble *Lsbgal*, when assayed with ONPG as substrate under standard conditions. Immobilization does not only shift the optimum temperature but it also broadens working temperature range. In

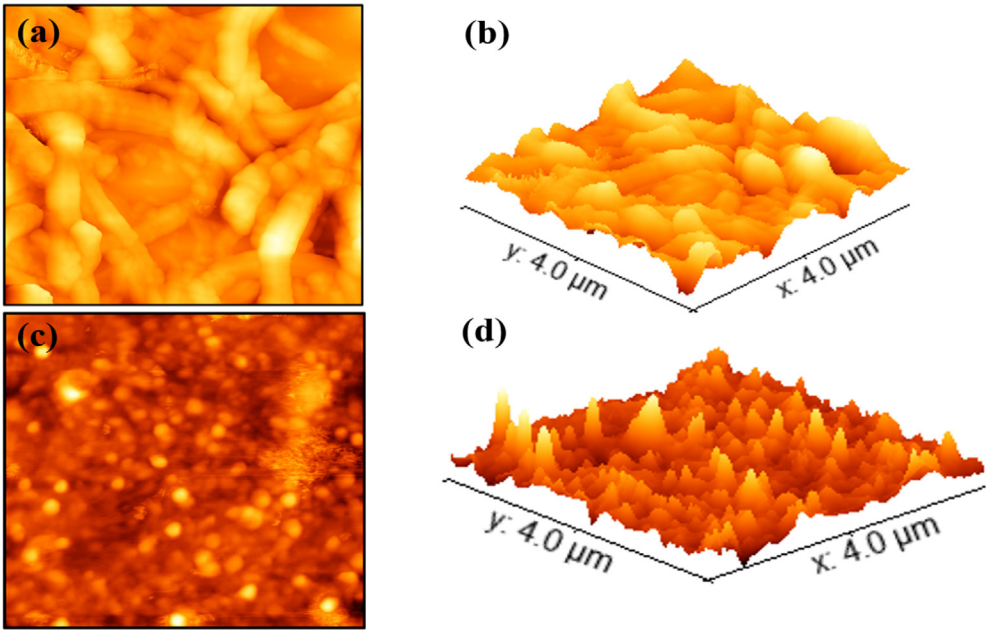

Fig. 3. (a) and (b) represents the 2-D and 3-D views of AFM images of bare MWCNT-MoS_2 NC respectively, (c) and (d) shows the 2-D and 3-D views of AFM images of enzyme immobilized MWCNT-MoS_2 NC, respectively.

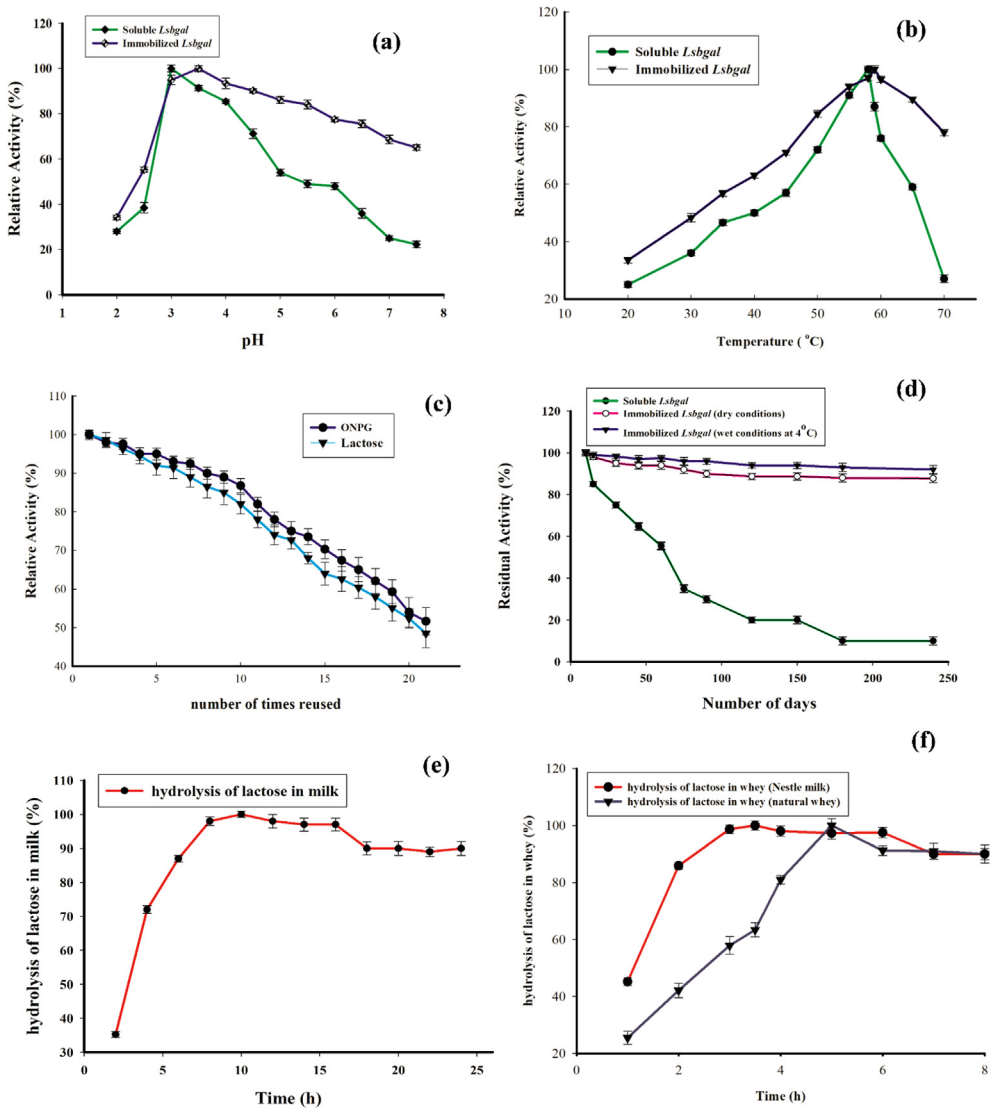

Fig. 4. (a) The effect of pH on the activity of soluble *vs* immobilized *Lsbgal* (b) effect of temperature (c) reusability of synthesized nanobiocatalyst for 21 times when assayed with ONPG and lactose as a substrate, respectively (d) storage stability of immobilized *Lsbgal* under wet (4 °C) and dry conditions compared with soluble *Lsbgal* (4 °C) (e) rate of milk lactose hydrolysis by immobilized *Lsbgal versus* time at room temperature. (f) rate of lactose hydrolysis in whey prepared from synthetic milk (Nestle) and natural whey by immobilized *Lsbgal versus* time at room temperature.

case of soluble *Lsbgal*, a sharp decline in activity was observed after 58 °C and had only 27% residual activity at 70 °C, while the immobilized *Lsbgal* retained 78% of residual activity at the same temperature [Fig. 4 (b)]. The reason behind the enhanced residual activity at higher temperature could be due the multisubunit multipoint covalent attachment of enzyme to nanocomposite induces the structural rigidification of enzyme, which prevent the unfolding of enzyme at higher temperature (Rodrigues et al., 2013). Similar changes in temperature optima were observed recently from our laboratory on *β*-amylase (Das, Talat, Srivastava, & Kayastha, 2018). The extent of shift in optimum temperature depends upon the type of interaction (ionic bond, covalent bond, etc.) between biocatalyst and nanocomposite.

3.3.3. Thermal stability

Thermal stability is the most decisive parameter from industrial point of view, because industrial conditions are not the same as enzyme conditions *in vivo*. An outstanding increase in thermal stability was observed in case of immobilized *Lsbgal*. The soluble *Lsbgal* showed thermal stability for only 5 min at 50 °C and 2 min at 55 °C with residual activity of 46% and 20%, respectively. However, the immobilized *Lsbgal* showed incredible increase in thermal stability for more than 8 h at 55 °C with retention of 94% of residual activity, when temperature increased to 60 °C, the immobilized *Lsbgal* showed thermal stability with residual activity of 75% for 2 h. However at 65 °C thermal stability was observed for 45 min with residual activity of 60% (data not shown). The remarkable increase in thermal stability after immobilization could be due to multisubunit covalent attachment of *Lsbgal* through residues present on its surface with nanocomposite *via* linker stabilizes the enzyme structure on support. Similarly, increase in thermal stability was observed in case *β*-galactosidase from *Bacillus circulans,* which retained 90% of residual activity when immobilized on macro-mesoporous modified siliceous support at 55 °C for 24 h (Bernal, Sierra, & Mesa, 2012).

3.3.4. Reusability and storage stability

Reusability are the benchmark parameter for selection of an enzyme for industrial utility because immobilization of enzyme doesn't only help in proficient recovery but it also permits reuse of expensive biocatalysts and thus determines the profitable economy for industrial utility. Immobilized *Lsbgal*, was reused for 21 times at its optimum

temperature and pH within 96 h. It retained 52% of the residual activity against ONPG up to 21 reuses, while in case of lactose, it retained 48.5% of residual activity for the same number of reuses [Fig. 4(c)]. The reason behind retention of activity for reuse, could be due to rigidification of enzyme structure by multisubunit multipoint covalent attachment, which enhances the stability of enzymes (Mateo et al., 2007). However, a loss in residual activity observed after each reuse of NBCs may be due to leaching of enzyme from nanomatrices, or may be due to distortion in active site of the enzyme by frequent encountering of the substrate. PANI/Co/MWCNTNC coupled *β*-galactosidase showed retention of 92% of residual activity after 10 successive reuses (Khan et al., 2017).

For enzyme producer, the knowledge of storage stability of enzyme has become extremely relevant for manufacturing of product to shipment of product to the end users. Storage stability study of *Lsbgal* revealed that NBCs showed excellent storage stability for 8 months with retention of 92% and 84% of residual activity under wet conditions (4 °C) and dry conditions (room temperature), respectively [Fig. 4(d)], while the soluble *Lsbgal* had retained only 42% of residual activity after 8 months at 4 °C and only 20% of residual activity at room temperature in one month (Data not shown). In a report, *β*-galactosidase immobilized on modified polypropylene membrane showed significant increase in storage stability up to 300th day with retention of 90% of residual activity (Vasileva, Iotov, Ivanov, Godjevargova, & Kotia, 2012). Immobilized *Lsbgal* showed an increase in stability of enzymes that may be attributed to multipoint covalent attachment of multisubunit enzyme to support, which reduces the proteolytic degradation of enzymes.

3.3.5. Determination of kinetic parameters

The kinetic parameter of *Lsbgal* were determined using Lineweaver-Burk plot to evaluate the catalytic performance after immobilization [Table 1]. After immobilization, the increase in K_m value was observed when compared with soluble enzyme, as it increased from 1.21 mM to 5.26 mM with ONPG, while in case of lactose it has showed an increase from 12.57 mM to 14.27 mM as outlined in [Table 1]. The increase in apparent K_m value after immobilization may be ascribed to strong multipoint covalent attachment of enzyme to support, which prevent the conformational changes. Recently, Das et al. (2017) have also reported an increase in K_m value after immobilization. The turnover number (k_{cat}) of immobilized *Lsbgal* was reduced as compared to soluble *Lsbgal* with both substrates i.e. ONPG and lactose that could be due to internal diffusion limitation of substrate to the enzyme rather than external diffusion rates (Zhang, Ge, & Liu, 2015).

3.3.6. Hydrolysis of lactose in milk and whey

The hydrolyzing capacities of synthesized NBCs, were tested at analytical scale in batch reactor. The rates of hydrolyzing capacity of immobilized *Lsbgal* for lactose in milk was found to be 10 h while in case of lactose in whey, the rate of hydrolysis was 3.5 h thereafter, it reaches the steady state as shown in [Fig. 4(e) & (f)]. When the hydrolysis was performed with lactose present in natural whey, the rate of hydrolysis was found to be 5 h. The hydrolysis of lactose in natural whey required more time as compared to prepared whey lactose from synthetic milk that could be possibly due to the presence of protecting components in natural whey. Immobilized *Lsbgal* showed good rate of hydrolysis in case of whey, because the pH optima of *Lsbgal* lies in an acidic range therefore it efficiently hydrolyzes the lactose in whey as compared to lactose in milk. Earlier, Kishore et al. (2012) have also reported similar pattern of hydrolysis of lactose in milk and whey. *Cicer arietinum* *β*-galactosidase immobilized onto graphene nanosheets exhibited milk and whey lactose hydrolysis in 5.17 h and 4.6 h, respectively. In the present study, good hydrolyzing capacities of the synthesized NBCs have made them as a promising candidate for the hydrolysis of lactose in dairy industry.

Table 1
Kinetic parameters for soluble and immobilized *Lsbgal* onto MWCNT-MoS_2 NC.

Enzyme preparations	k_{cat} ($\times 10^5$ sec^{-1})	K_m (mM)	k_{cat}/K_m ($\times 10^4$ $mM^{-1}s^{-1}$)
Soluble *Lsbgal* (ONPG)	1.02 ± 0.06	1.21 ± 0.03	8.42 ± 0.14
Immobilized *Lsbgal* (ONPG)	0.36 ± 0.09	5.26 ± 0.05	0.68 ± 0.24
Soluble *Lsbgal* (Lactose)	1.64 ± 0.14	12.57 ± 0.12	1.30 ± 0.12
Immobilized *Lsbgal* (Lactose)	0.34 ± 0.32	14.27 ± 0.56	0.23 ± 0.03

3.3.7. Effect of galactose and glucose

Product inhibition is one of the serious drawbacks from the industrial viewpoint. The stability of soluble and immobilized *Lsbgal* in the presence of increasing concentration of glucose and galactose have been carried out [Fig. S8] supplementary file. The immobilized *Lsbgal* was found to be more resistant against galactose inhibition as it retained 65% of activity at 50 mM galactose while, soluble *Lsbgal* retained only 20% of activity, under similar conditions; while glucose does not significantly inhibit the activity of *Lsbgal* in case of soluble and immobilized even up to 70 mM of glucose concentration. The most probable reason behind the decreased inhibition in case of immobilized *Lsbgal* could be due to multipoint covalent attachment of enzyme to heterofunctional support that lowers the interaction of inhibitor with the enzyme (Mateo et al., 2007). Pessela et al. (2003) have investigated reduced inhibition and showed 4 fold increase in K_i when *β*-galactosidase from *Thermus* sp. was immobilized on heterofunctional epoxy activated Sephabeads when compared to its soluble counterpart.

4. Conclusion

In the present study, we have shown a successful synthesis of 3D MWCNT-MoS_2 NC *via* hydrothermal method, which is cost-effective, eco-friendly, and heterofunctional in nature. Heterofunctional MWCNT-MoS_2 NC was used as platform to immobilization of *Lsbgal*. A simple method of immobilization of glutaraldehyde linking chemistry resulted in 93% immobilization efficiency. The synthesized nanobiocatalyst showed alteration in kinetic parameters and offered superiority over soluble *Lsbgal*. However, NBCs showed broadening in pH, temperature working range along with excellent storage stability up to 8 months with retention of 92% of residual activity at 4 °C. NBCs showed excellent reusability as it retained ~50% of residual activity up to 21 reuses. It also hydrolyzes whey lactose efficiently as compared to milk lactose. These properties of NBCs make it an auspicious contender for effective hydrolysis of whey lactose and lactose containing products in dairy industry. On the other hand, these heterofunctional nanomatrices can serve as a novel platform for construction of stable nanobiosensor by multipoint covalent attachment to detect hidden lactose present in prescription drugs and a variety of dairy products. 3D nanocomposite can be used as matrix for other industrially important enzymes.

Acknowledgements

Anjali Yadav sincerely expresses her thanks to UGC (NF-OBC), New Delhi for providing financial support in form of Junior and Senior Research Fellowship (F./2015-16/NFO-2015-17-OBC-UTT-32658/ (SA-III-website). Himanshu Mishra is thankful to CSIR, New Delhi for providing SRF fellowship (Letter No.: 09/013 (0752)/2018-EMR-I). Sumit Kumar Pandey is thankful to UGC for providing fellowship. Anchal Srivastava is thankful to SERB, India (Project Code: EMR/2016/007720), DST-PURSE and CAS-BHU for providing financial assistance.

Declaration of Competing Interest

The authors declare no competing financial interest.

Appendix A. Supplementary data

Supplementary data to this article can be found online at https://doi.org/10.1016/j.foodchem.2019.125005.

References

Adam, A. C., Rubio-Texeira, M., & Polaina, J. (2005). Lactose: The milk sugar from a biotechnological perspective. *Critical Reviews in Food Science and Nutrition, 44*, 553–557.

Atkinson, R. L., Kratzer, F. H., & Stewart, G. F. (1957). Lactose in animal and human feeding: A review. *Journal of Dairy Science, 40*, 1114–1132.

Barbosa, O., Ortiz, C., Berenguer-Murcia, Á., Torres, R., Rodrigues, R. C., & Fernandez-Lafuente, R. (2014). Glutaraldehyde in bio-catalysts design: A useful crosslinker and a versatile tool in enzyme immobilization. *RSC Advances, 4*, 1583–1600.

Barbosa, O., Torres, R., Ortiz, C., Berenguer-Murcia, Á., Rodrigues, R. C., & Fernandez-Lafuente, R. (2013). Heterofunctional supports in enzyme immobilization: From traditional immobilization protocols to opportunities in tuning enzyme properties. *Biomacromolecules, 14*, 2433–2462.

Bernal, C., Sierra, L., & Mesa, M. (2012). Improvement of thermal stability of *β*-galactosidase from *Bacillus circulans* by multipoint covalent immobilization in hierarchical macro-mesoporous silica. *Journal of Molecular Catalysis B: Enzymatic, 84*, 166–172.

Bezerra, M. A., Santelli, R. E., Oliveira, E. P., Villar, L. S., & Escaleira, L. A. (2008). Response surface methodology (RSM) as a tool for optimization in analytical chemistry. *Talanta, 76*, 965–977.

Bradford, M. M. (1976). A rapid and sensitive method for the quantitation of microgram quantities of protein utilizing the principle of protein-dye binding. *Analytical Biochemistry, 72*, 248–254.

Chou, S. S., De, M., Kim, J., Byun, S., Dykstra, C., Yu, J., ... Dravid, V. P. (2013). Ligand conjugation of chemically exfoliated MoS_2. *Journal of American Chemical Society, 135*, 4584–4587.

Das, R., Mishra, H., Srivastava, A., & Kayastha, A. M. (2017). Covalent immobilization of *β*-amylase onto functionalized molybdenum sulfide nanosheets, its kinetics and stability studies: A gateway to boost enzyme application. *Chemical Engineering Journal, 328*, 215–227.

Das, R., Talat, M., Srivastava, O. N., & Kayastha, A. M. (2018). Covalent immobilization of peanut *β*-amylase for producing industrial nano-biocatalysts: A comparative study of kinetics, stability and reusability of the immobilized enzyme. *Food Chemistry, 245*, 488–499.

Deep, A., Tiwari, U., Kumar, P., Mishra, V., Jain, S. C., Singh, N., ... Bharadwaj, L. M. (2012). Immobilization of enzyme on long period grating fibers for sensitive glucose detection. *Biosensors & Bioelectronics, 33*, 190–195.

DiCosimo, R., McAuliffe, J., Poulose, A. J., & Bohlmann, G. (2013). Industrial use of immobilized enzymes. *Chemical Society Reviews, 42*(15), 6437–6474.

Dwevedi, A., & Kayastha, A. M. (2009). Optimal immobilization of beta-galactosidase from Pea (PsBGAL) onto Sephadex and chitosan beads using response surface methodology and its applications. *Bioresource Technology, 100*, 2667–2675.

Geiger, B., Nguyen, H.-M., Wenig, S., Nguyen, H. A., Lorenz, C., Kittl, R., ... Nguyen, T.-H. (2016). From by-product to valuable components: Efficient enzymatic conversion of lactose in whey using *β*-galactosidase from *Streptococcus thermophilus*. *Biochemical Engineering Journal, 116*, 45–53.

González Siso, M. I. (1996). The biotechnological utilization of cheese whey: A review. *Bioresource Technology, 57*, 1–11.

Khan, M., Husain, Q., & Bushra, R. (2017). Immobilization of *β*-galactosidase on surface modified cobalt/multiwalled carbon nanotube nanocomposite improves enzyme stability and resistance to inhibitor. *International Journal of Biological Macromolecules, 105*, 693–701.

Kim, J., Grate, J. W., & Wang, P. (2008). Nanobiocatalysis and its potential applications. *Trends in Biotechnology, 26*, 639–646.

Kishore, D., Talat, M., Srivastava, O. N., & Kayastha, A. M. (2012). Immobilization of *β*-galactosidase onto functionalized graphene nano-sheets using response surface methodology and its analytical applications. *PloS One, 7*, e40708.

Lehman, J. H., Terrones, M., Mansfield, E., Hurst, K. E., & Meunier, V. (2011). Evaluating the characteristics of multiwall carbon nanotubes. *Carbon, 49*, 2581–2602.

Liu, Y., Yu, D., Zeng, C., Miao, Z., & Dai, L. (2010). Biocompatible graphene oxide-based glucose biosensors. *Langmuir, 26*, 6158–6160.

Mahoney, R. R. (1998). Galactosyl-oligosaccharide formation during lactose hydrolysis: A review. *Food Chemistry, 63*, 147–154.

Mateo, C., Palomo, J. M., Fernandez-Lorente, G., Guisan, J. M., & Fernandez-Lafuente, R. (2007). Improvement of enzyme activity, stability and selectivity *via* immobilization techniques. *Enzyme and Microbial Technology, 40*, 1451–1463.

Melo, R. R.d, Alnoch, R. C., Vilela, A. F. L., Souza, E. M.d., Krieger, N., Ruller, R., Sato, H. H., & Mateo, C. (2017). New Heterofunctional supports based on glutaraldehyde-activation: A tool for enzyme immobilization at neutral pH. *Molecules (Basel, Switzerland), 22*, 1088.

Monsan, P. (1978). Optimization of glutaraldehyde activation of a support for enzyme immobilization. *Journal of Molecular Catalysis, 3*, 371–384.

Pan, C., Hu, B., Li, W., Sun, Y., Ye, H., & Zeng, X. (2009). Novel and efficient method for immobilization and stabilization of *β*-d-galactosidase by covalent attachment onto magnetic Fe_3O_4–chitosan nanoparticles. *Journal of Molecular Catalysis B: Enzymatic, 61*, 208–215.

Perumal Veeramalai, C., Li, F., Xu, H., Kim, T. W., & Guo, T. (2015). One pot hydrothermal synthesis of graphene like MoS_2 nanosheets for application in high performance lithium ion batteries. *RSC Advances, 5*, 57666–57670.

Pessela, B. C. C., Mateo, C., Fuentes, M., Vian, A., García, J. L., Carrascosa, A. V., Guisán, J. M., & Fernández-Lafuente, R. (2003). The immobilization of a thermophilic *β*-galactosidase on Sepabeads supports decreases product inhibition: Complete hydrolysis of lactose in dairy products. *Enzyme and Microbial Technology, 33*(2), 199–205.

Richmond, M., Gray, J., & Stine, C. (1981). Beta-galactosidase: Review of recent research related to technological application, nutritional concerns, and immobilization. *Journal of Dairy Science, 64*, 1759–1771.

Rodrigues, R. C., Ortiz, C., Berenguer-Murcia, A., Torres, R., & Fernandez-Lafuente, R. (2013). Modifying enzyme activity and selectivity by immobilization. *Chemical Society Review, 42*, 6290–6307.

Shan, C., Yang, H., Song, J., Han, D., Ivaska, A., & Niu, L. (2009). Direct electrochemistry of glucose oxidase and biosensing for glucose based on graphene. *Analytical Chemistry, 81*, 2378–2382.

Shouzhi, W., Jiayan, Z., Yongliang, S., Weiran, L., Yongzhong, W., Lei, Z., & Xiaopeng, H. (2017). Three-dimensional MoS_2@CNT/RGO network composites for high-performance flexible supercapacitors. *Chemistry – A European Journal, 23*, 3438–3446.

Shukla, T. P., & Wierzbicki, L. E. (1975). Beta-galactosidase technology: A solution to the lactose problem. *C R C Critical Reviews in Food Technology, 5*, 325–356.

Singh, V. K., Kumar, S., Pandey, S. K., Srivastava, S., Mishra, M., Gupta, G., ... Srivastava, A. (2018). Fabrication of sensitive bioelectrode based on atomically thin CVD grown graphene for cancer biomarker detection. *Biosensors & Bioelectronics, 105*, 173–181.

Srivastava, A., Srivastava, O. N., Talapatra, S., Vajtai, R., & Ajayan, P. M. (2004). Carbon nanotube filters. *Nature Materials, 3*, 610–614.

Talat, M., Awasthi, K., Sundar, S., & Srivastava, O. N. (2015). Functionalization of carbon nanomaterials (e.g. carbon nanotubes and graphene) using L-cysteine. *Innovations in Corrosion and Materials Science (Formerly Recent Patents on Corrosion Science), 5*(2), 105–112.

Vasileva, N., Iotov, V., Ivanov, Y., Godjevargova, T., & Kotia, N. (2012). Immobilization of *β*-galactosidase on modified polypropilene membranes. *International Journal of Biological Macromolecules, 51*, 710–719.

Wang, Y., & Ni, Y. (2014). Molybdenum disulfide quantum dots as a photoluminescence sensing platform for 2,4,6-trinitrophenol detection. *Analytical Chemistry, 86*, 7463–7470.

Wohlgemuth, R. (2010). Biocatalysis—key to sustainable industrial chemistry. *Current Opinion in Biotechnology, 21*, 713–724.

Xiao, Z., Xie, Y., Militz, H., & Mai, C. (2010). Effect of glutaraldehyde on water related properties of solid wood. *Holzforschung, 64*, 483–488.

Zaak, H., Sassi, M., & Fernandez-Lafuente, R. (2018). A new heterofunctional amino-vinyl sulfone support to immobilize enzymes: Application to the stabilization of *β*-galactosidase from *Aspergillus oryzae*. *Process Biochemistry, 64*, 200–205.

Zhang, Y., Ge, J., & Liu, Z. (2015). Enhanced activity of immobilized or chemically modified enzymes. *ACS Catalysis, 5*(8), 4503–4513.